Vacancy self-diffusion parameters in tungsten: Finite electron-temperature LDA calculations

Alessandra Satta
Section de Recherches de Métallurgie Physique, CEA/Saclay, 91191 Gif-sur-Yvette, France and Istituto Nazionale per la Fisica della Materia (INFM) and Dipartimento di Scienze Fisiche, Universitá di Cagliari, via Ospedale 72, 09124 Cagliari, Italy

F. Willaime
Section de Recherches de Métallurgie Physique, CEA/Saclay, 91191 Gif-sur-Yvette, France

Stefano de Gironcoli
Istituto Nazionale per la Fisica della Materia (INFM) and Scuola Internazionale Superiore di Studı Avanzati (SISSA) via Beirut 2-4, 34014 Trieste, Italy

(Received 9 October 1997)

An *ab initio* pseudopotential study of the monovacancy properties in bcc tungsten is presented. The formation and migration enthalpies are calculated for relaxed configurations using supercells containing up to 54 atomic sites, both in the electronic ground state and at finite electron temperature. The electronic contribution to the formation entropy — usually neglected in point defect calculations — is shown to be positive and equal to $1.74k_B$ at melting temperature. This large value is related to peaks in the electronic density of states just below the Fermi level due to states localized around the vacancy. The calculated values of the migration and formation enthalpies are found to be in excellent agreement with experiments at low temperatures, and their significant quadratic temperature dependence — due to electronic excitations — is shown to explain part of the experimentally observed temperature dependence of the migration enthalpy and self-diffusion activation energy. The tracer self-diffusion coefficient is calculated within the rate theory: the Arrhenius slope is in excellent agreement with experiments, and so are the absolute values provided that the electronic entropies are taken into account. [S0163-1829(98)03518-8]

I. INTRODUCTION

The self-diffusion behavior in pure metals is usually discussed as a function of the crystal structure and a universal understanding of diffusion mechanisms in bcc metals is still lacking.[1] In fcc metals, the monovacancy mechanism is confirmed to be dominant at low temperatures, and two explanations concerning the exact origin of the weak curvature found in the Arrhenius plot of the self-diffusion coefficient are still under discussion: temperature dependence of the self-diffusion parameters or dominance of the divacancy mechanism at high temperatures.[2] In bcc metals, the situation is more complex and is characterized by the following features:

(1) The average self-diffusion activation energy shows pronounced group-specific tendencies: its value normalized to the melting temperature or to the cohesive energy increases strongly when going from group IV elements ($\beta-$Ti, $\beta-$Zr, $\beta-$Hf) to groups V (V, Nb, Ta), and VI (Cr, Mo, W).[3] The behavior of alkali metals (Li, Na, K) is intermediate between that of group IV and group V elements.
(2) The activation energy has a significant temperature dependence, i.e., the Arrhenius plots of the self-diffusion coefficients are strongly curved, with the exception of Cr (Ref. 3).
(3) For most elements, reliable experimental data of the formation and migration energies for the vacancy mechanism are lacking.[4]

The dominant mechanism at low temperatures, which may not be the same for all bcc elements, is not firmly established. Several models have been proposed in the past, including direct exchange or ring mechanism,[5] but most of the recent explanations focus on the simple monovacancy mechanism. A group dependence of the vacancy migration energy was proposed in relation with phonon properties[3,6] suggesting that the abnormally fast diffusion in group IV elements at low temperatures is *partly* governed by the pronounced softening of the LA $2/3\,\langle 111\rangle$ and the N-T_1 $\langle 110\rangle$ phonon modes. However the fast migration of the vacancy alone is not sufficient to explain why self-diffusion is six orders of magnitude faster in group IV elements than in group VI elements at half the melting temperature. Quantitative analyses indeed show that this behavior can be understood within the vacancy mechanism only if the vacancy concentration is also strongly group dependent.

The origin of the pronounced curvature remains the other main open question. The contribution of two competing mechanisms, such as divacancies, next-nearest-neighbor jumps of the monovacancy, or self-interstitials, in addition to the most likely monovacancy mechanism, has been widely discussed.[3] The most recent evidences promote the concept of monovacancy model with temperature-dependent activation energy.[2,7,8] The unusual temperature dependence of the frequencies of specific phonon modes recorded in bcc transition metals also supports the idea of a temperature dependence of vacancy-migration parameters.[6]

In the context described above, atomistic calculations may help to elucidate the energetics and dynamics of defect formation and migration in bcc metals. In alkali metals, new diffusion mechanisms were proposed at high temperatures in sodium, based upon molecular-dynamics simulations using semiempirical interatomic potentials: vacancy double jumps[9] and ring-exchange mechanisms.[10] To conclude on the low-temperature mechanism, semiempirical potentials[11] are not reliable enough and first-principles electronic structure calculations of defect parameters, performed in Li and Na, showed that the interstitialcy mechanism can be excluded and that the calculated vacancy formation energy is very close to the experimental activation energy.[12,13] Moreover, in Li, a very low vacancy migration energy was found, and the self-diffusion coefficient for the monovacancy mechanism, calculated within the transition state theory (TST),[14,15] including the calculation of the vibrational formation entropy in the harmonic approximation, gives a very good agreement with experimental data.[16] These results strongly support the vacancy mechanism in Li.

As for transition metals, semiempirical potentials, derived from the embedded-atom method or the second moment approximation, can give a first estimate of defect parameters.[17–21] In particular, unlike pair potentials, they give realistic values of the vacancy formation energies. However, these potentials are less satisfactory in bcc metals than in fcc metals, in particular in groups V and VI where angular forces, which are missing in these models, are known to be important. The properties of bcc transition metals are indeed governed by the characteristic bimodal shape of the electronic density of states. This feature is very well reproduced by simple *d*-band tight-binding models, which were successfully used to study the trends of the vacancy formation energy in the bcc structure along a transition-metal series.[22,23] These calculations showed a strong group dependence, related to the position of the Fermi level with respect to the minimum of the pseudogap.[23,24] Very few first-principles electronic structure calculations of the vacancy formation energy were performed in transition metals. The results reported using the Korringa-Kohn-Rostoker method[25] or the full potential linear muffin-tin orbital (FP-LMTO) method[26] are in good agreement with experiments in fcc metals. The agreement is less satisfactory in bcc metals, in particular in V, Cr, and Ta where the calculated results are typically 25 to 50 % higher than the recommended experimental values. The relaxation energies, which were not taken into account, are not sufficient to explain this difference. Further investigations are necessary to understand these discrepancies.

In this paper we present first-principles density-functional calculations of the self-diffusion parameters for the monovacancy mechanism in bcc tungsten. Tungsten was chosen because a large body of information is available both on diffusion data[27] and on vacancy parameters.[8,28,29] Quenched-in resistivity and annealing experiments showed that the sum of the vacancy formation enthalpy $H^f = 3.67 \pm 0.2$ eV and the vacancy migration enthalpy $H^m = 1.78 \pm 0.1$ eV (Ref. 28) was in very good agreement with the activation enthalpy $Q_1 = 5.45$ eV for the low temperature process.[27] On the basis of these results it was concluded that the monovacancy mechanism is dominant at low temperatures (at least up to 2/3 of the melting temperature). Corrections[30] and new analyses[31] of these data showed that this exceptional agreement needs to be revised. Moreover it was then shown that the migration enthalpy was temperature dependent.[8]

The organization of the paper is as follows. In Sec. II, the definitions of the self-diffusion parameters are recalled, and the theory of their temperature dependence is formulated including electron-temperature effects. The computational details used in the present finite-temperature local-density-approximation (LDA) calculations and super-cell approach for defect calculations are described in Sec. III. In Sec. IV, the results of the relaxed vacancy formation and migration enthalpies and entropies as function of the electron temperature are presented. The comparison with experiments is discussed, and the origin of the large value of the electronic entropy contributions are analyzed from peaks in the density of states. Finally the tracer self-diffusion coefficient is calculated with the transition state theory and compared with experimental data.

II. THERMODYNAMICS OF DEFECT PARAMETERS

A. Formation parameters

The vacancy concentration at thermal equilibrium in a crystal $C_{\mathrm{eq}}(T)$ is given by

$$C_{\mathrm{eq}}(T) = \exp\left(- \frac{G^f}{k_B T} \right). \tag{1}$$

All the vacancy formation functions at constant pressure, namely the Gibbs energy G^f, the enthalpy H^f, and the entropy S^f, are defined as differences of the corresponding functions taken between a perfect crystal and a crystal with one vacancy.[7] Therefore their temperature dependences can be understood from the two main contributions to the entropy of a crystal, namely, the vibrational term S_{vib}, and the electronic excitation term S_{el}:[32]

$$S = S_{\mathrm{el}} + S_{\mathrm{vib}}. \tag{2}$$

Since S_{el} is smaller than S_{vib} by typically two orders of magnitude or more at high temperatures, it is often omitted. This is in particular the case for defect parameters, where the electronic contribution of the vacancy formation entropy S^f_{el} is only rarely mentioned.[33] However, when considering *differences* between two atomic configurations, ΔS_{el} can be comparable to ΔS_{vib}. It is for instance the case between different crystallographic structures in transition metals,[43] and as demonstrated below, it can also be the case for defect parameters. The vibrational contribution to the vacancy formation entropy S^f_{vib}, can be calculated in the harmonic approximation.[33] These types of calculations have recently been achieved in Li using electronic structure calculations.[16] Typical calculated values range from 1 to $4k_B$. A first estimate of S_{el} in a metal is given by the low-temperature development in a free-electron gas model:

$$S_{\mathrm{el}}(T) \simeq \frac{1}{3} \pi^2 n(E_F) k_B T. \tag{3}$$

Larger values of S_{el} are reached in transition metals compared to other metals because both the density of states at the Fermi level $n(E_F)$ and the melting temperature are higher. An important consequence of Eq. (3) is that if the local density of states at the Fermi level changes significantly close to the vacancy with respect to the bulk value, high absolute values of S^f_{el} are expected. In order to discuss the temperature dependence of H^f, which is related to that of S^f, through[7]

$$\left(\frac{\partial H^f}{\partial T}\right) = T\left(\frac{\partial S^f}{\partial T}\right), \tag{4}$$

it is useful to write H^f as the sum of three terms, which are obtained by integrating Eq. (4) and using Eq. (2):

$$H^f(T) = H^f(0) + \Delta H^f_{el}(T) + \Delta H^f_{vib}(T). \tag{5}$$

At high temperature the ions behave classically and, in the harmonic approximation, each normal mode contributes as $k_B T$ to the enthalpy and therefore ΔH^f_{vib} vanishes and S^f_{vib} is temperature independent. On the other hand, the linear temperature dependence which is qualitatively expected for S^f_{el} from Eq. (3) leads to a quadratic temperature dependence of $\Delta H^f_{el}(T)$ and of $\Delta G^f_{el}(T)$, defined as

$$\Delta G^f_{el}(T) = \Delta H^f_{el}(T) - T S^f_{el}(T). \tag{6}$$

B. Migration and self-diffusion parameters

Let us recall the formalisms and approximations which allow us to define migration parameters, similar to the thermodynamically well-defined formation parameters. Two theories, namely the rate theory[14] and the dynamical theory,[15] were proposed to show that the vacancy jump rate $\Gamma(T)$ has an Arrhenius form:

$$\Gamma(T) = \Gamma_0 \exp\left(-\frac{Q^m}{k_B T}\right). \tag{7}$$

The potential-energy surface considered in these theories for the motion of the ions, is that given in the present electronic-structure calculations, by the free energy with respect to electronic degrees of freedom F_{el}:

$$F_{el}(T_{el}) = E_{el}(T_{el}) - T_{el} S_{el}(T_{el}), \tag{8}$$

where $E_{el}(T_{el})$ is the internal energy at finite electron temperature T_{el}. It was shown that migration parameters which are compatible with these two theories can be defined under reasonable approximations.[7] This consists in taking $\Gamma_0 = \sqrt{\frac{3}{5}}\nu_D$, where ν_D is the Debye frequency, and a vibrational migration entropy S^m_{vib}, which can be formally defined in the rate theory, equal to zero. The energy Q^m in Eq. (7) is then equal to the potential-energy difference ΔF_{el} between the saddle-point configuration and the initial configuration. For simplicity, all the migration functions will be taken here at constant pressure. The migration enthalpy is defined by $H^m = \Delta F_{el}$, and the migration entropy S^m reduces to the electronic contribution, since $S^m_{vib} = 0$. Therefore the temperature dependences of H^m and S^m are related, as if they were true thermodynamical functions as in Eq. (4).

The tracer self-diffusion coefficient for a monovacancy mechanism with nearest-neighbor jumps is given by

$$D^*(T) = \frac{1}{6} Z \delta^2 f C_{eq}(T) \Gamma(T), \tag{9}$$

where Z and δ are, respectively, the number of nearest neighbors and the jump length. The tracer correlation factor f, which accounts for the fact that atomic jumps are not independent, is equal to 0.78 for a vacancy mechanism in a bcc structure.[1] The activation functions — Gibbs energy G^a enthalpy H^a, and entropy S^a — for the monovacancy mechanism are defined as equal to the sum of the corresponding formation and migration functions. The important point is that the use of a finite electron-temperature formalism does not change the fact that the temperature-dependent Arrhenius slope of D^*, is equal to the negative of the activation enthalpy:

$$\frac{\partial \ln D^*}{\partial \beta} = -H^a, \tag{10}$$

where $\beta = (k_B T)^{-1}$ with T taken as the temperature of both the electrons and the ions.

III. COMPUTATIONAL PROCEDURE

The present self-consistent electronic structure-calculations are performed within the framework of the density-functional theory in the local-density approximation (DFT-LDA), using norm-conserving pseudopotentials[34] and plane-wave basis sets. For W we use a standard pseudopotential[35] that has previously been successfully applied to the study of surface phonons.[36] A kinetic-energy cutoff of 30 Ry is sufficient to converge all the quantities of interest, as checked by increasing the cutoff up to 40 Ry in test calculations performed on the smallest (16-site) supercells. Special k points are used for the Brillouin-zone (BZ) sampling.[37] The density of k points used in the present calculations is at least equivalent to that of 112 special k points in a one atom supercell (see Sec. IV).

A. Ground-state and finite electron-temperature calculations

The generalization of the Hohenberg-Kohn theorem to finite temperatures[38–40] is used to investigate the effect of electron temperature on the self-diffusion parameters. The occupation numbers of the single-particle Kohn-Sham orbitals f_i are given by the Fermi distribution function, and the electronic entropy S_{el} is calculated, neglecting the entropy contributions arising from the exchange and correlation potentials,[41] as[40,32]

$$S_{el} = -2k_B \sum_i \left[f_i \ln f_i + (1-f_i)\ln(1-f_i)\right]. \tag{11}$$

This formalism was successfully applied to study the electronic contribution to the bulk entropy of transition metals.[32,42,43] In the present study, we have examined only the electronic contributions to the entropies and the free energies, and not the vibrational contributions. Concerning the ground-state properties, i.e., the $T \to 0$ limit, this approach is no longer practical, as a prohibitively large number of k points would be needed. We therefore resorted to the smear-

ing technique using the Hermite-Gauss function of order 1 (Refs. 44, 45), and a smearing width $\sigma = 20$ mRy.

B. Defect calculations

The calculations are performed using the supercell geometry. The repeating cell must be large enough to make the interaction between the defects negligible. All quantities are calculated at zero pressure, i.e., the free energy of the system is minimized with respect to the supercell volume. Denoting $E(N,\nu,\Omega)$, the energy of the system of N atoms and ν vacancies, occupying $N+\nu$ sites in volume Ω, the vacancy formation enthalpy at zero pressure H^f is[40]

$$H^f = E[N-1,1;\Omega(N-1,1;0)] - \frac{N-1}{N}E(N,0;N\Omega_0), \tag{12}$$

where Ω_0 is the bulk equilibrium atomic volume, and $\Omega(N,\nu;P)$ is the equilibrium volume of the system of N atoms and ν vacancies at pressure P. The vacancy formation volume Ω^f is obtained from $\Omega(N-1,1;0)$, appearing in Eq. (12), through

$$\Omega^f = \Omega(N-1,1;0) - (N-1)\Omega_0. \tag{13}$$

The electronic contribution to the vacancy formation entropy at zero pressure $S^f_{\rm el}$ is obtained by replacing energies by entropies in Eq. (12). The relaxation procedure is performed iteratively in two steps. First, the structure is relaxed at fixed volume, by minimizing the total energy with respect to the positions of all atoms until the Hellmann-Feynman forces vanish. Then, the volume is relaxed, with atomic positions within the supercell being held fixed. A further structural and volume relaxation did not yield significant changes in the total energy of the system (less than 0.01 eV), and only weak changes in the equilibrium volumes ($\approx 0.01\Omega_0$). For the calculation of migration parameters, the unrelaxed saddle-point configuration is obtained when an atom is displaced halfway in the $\langle 111\rangle$ direction towards the vacancy. By relaxing the position of all atoms, except the migrating atom, as well as the volume, the relaxed saddle-point configuration is reached. The migration volume Ω^m at zero pressure is defined as the volume difference between the equilibrium volumes of the saddle-point configuration and the initial configuration. The defect energies have been defined above in the isobaric ensemble. The equivalent energies are slightly different when calculated in the isochoric ensemble, i.e., at fixed volume *per atom*,[46] or at fixed supercell size. At zero pressure, they are all equal in the thermodynamic limit, $N\to\infty$. For the supercell with $N=16$ sites, the difference between fixed supercell size and constant pressure results is found here to be of the order of 0.2 eV for the formation energy and 0.05 eV for the migration energy. This difference is expected to decrease as $1/N$ (Ref. 46). The results presented below focus on the isobaric calculations because this corresponds to the experimental situation, but also because the convergence with respect to supercell size is found to be faster.

TABLE I. Calculated formation H^f, migration H^m, and self-diffusion H^a enthalpies, in fully relaxed configurations (positions and volumes) at zero temperature. The unrelaxed energies calculated at constant supercell volume are given in parentheses for comparison. N denotes the number of atomic sites in the supercell. The number of inequivalent k points used in the BZ integration, n_k, refers to the initial mesh in the cubic symmetry; for the saddle-point configuration, due to the lower symmetry, the actual number of k points is larger.

	N	n_k	H^f (eV)	H^m (eV)	H^a (eV)
Present work	16	10	3.76 (4.04)	1.70 (1.95)	5.46 (5.99)
	27	8	3.69 (3.88)	1.69 (2.08)	5.38 (5.96)
	27	14	3.77	1.71	5.48
	54	4	3.44 (3.68)	1.82 (2.06)	5.26 (5.74)
FP-LMTO[a]	27	16	(3.27)		

[a]Reference 26.

IV. RESULTS

A. Ground-state energies

The formation and the migration enthalpies and volumes, for the ground-state electronic configuration, have been calculated for supercells with increasing numbers of sites N (16, 27, and 54), and various numbers of inequivalent k points, n_k. The convergence as function of supercell size and Brillouin-zone sampling is one of the major problems in order to obtain meaningful results for defect parameters from electronic-structure calculations in metals due to computational limitations.[12] The energy results at zero temperature are summarized in Table I, both for the unrelaxed and fully relaxed configurations. The density of k points in the supercell BZ is the same for $N=16$, 27, and 54 when $n_k=10$, 8, and 4, respectively. Test calculations performed on the $N=16$ supercell with $n_k=10$ or 20 and different smearing width ($\sigma=20$ or 70 mRy) lead exactly to the same value of the unrelaxed vacancy formation energy within 0.01 eV. In view of the difference between the $n_k=8$ and $n_k=14$ calculations for $N=27$, the results can be considered to be converged with respect to n_k within approximately 0.1 eV for this particular density of k points. As for the convergence with respect to system size, it is expected to be much smaller than that between the $N=27$ and $N=54$ results, i.e., 0.2 eV, and is found to be faster in relative values than for alkali metals.[12]

A vacancy formation energy of $E^f=3.27$ eV was previously reported for tungsten using the FP-LMTO technique without relaxation at fixed supercell size.[26] This value is significantly lower, by 0.6 eV, than the present result for the same supercell size and equivalent k-point density. Part of the discrepancy may be due to the Gaussian-broadening scheme used in Ref. 26. The general discrepancy between the calculated and experimental values of vacancy formation energies in bcc metals observed in Ref. 26 is suggested to be due to the insufficient size of the basis set which was used, in particular since only two values of the kinetic energy—instead of three in the most recent calculations—were used for the Hankel functions of the s and p orbitals.[47]

The effect of atomic relaxation at fixed supercell size, is found to reduce the energy by only ~ 0.1 eV. The amplitudes

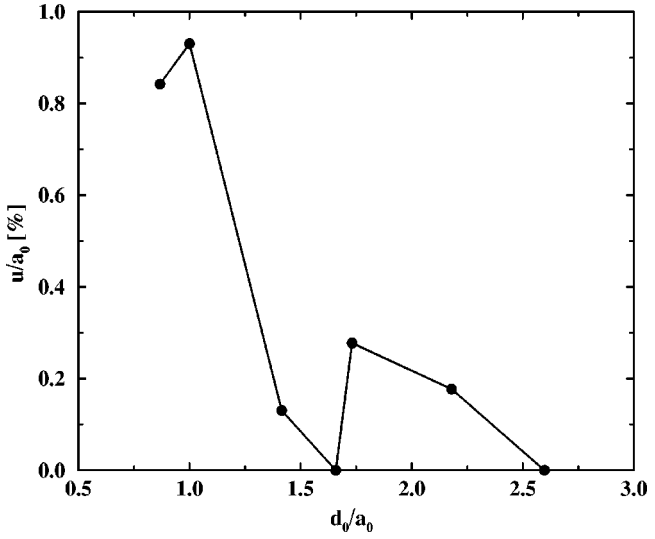

FIG. 1. Amplitude of the atomic relaxations u as function of the distance to the vacancy, d_0. Results correspond to the $N=54$ supercell calculation at fixed supercell size. Distances are normalized to the bulk lattice parameter a_0.

of the displacements are small (see Fig. 1): they are in the lower range of what is typically found for bcc-transition metals with semiempirical potentials[48] but one order of magnitude smaller than the *ab initio* results reported for Li.[12] Stiffer force constants may be at the origin of these small displacements. A surprising feature is that *all* atoms, i.e., including second nearest neighbors of the vacancy, are found to have *inward* relaxations. At the saddle-point configuration, the relaxation energy due to atomic displacements is larger (≈ 0.4 eV), and can therefore not be neglected. The formation and migration volumes are listed in Table II. The formation volume is found to be quite independent of the system size.

B. Temperature dependence

The calculation of the temperature dependence of enthalpies and electronic entropies is performed according to the formalism described in Sec. III A. The calculated bulk electronic entropies are in excellent agreement with previous calculations.[32] The results for the electronic contribution to the vacancy migration $S^m_{\rm el}$ formation $S^f_{\rm el}$, and activation $S^a_{\rm el}$ entropies presented in Fig. 2(a) for three different temperatures $T=1579$, 2526, and 3679 K are found to depend essentially linearly on temperature, as expected from Eq. (3). Both $S^m_{\rm el}$ and $S^f_{\rm el}$ are positive, reaching values of 0.52 and $1.74k_B$, respectively, at the melting temperature of tungsten, $T_m=3683$ K. These values are not negligible compared to typical values of the vibrational contribution to the formation entropy $S^f_{\rm vib}$. As will become clear in Sec. IV C, the calculated values of $S^m_{\rm el}$ and $S^f_{\rm el}$ are very sensitive to the description of the density of states close to the Fermi level, as well as to the position of the Fermi level itself. The results are therefore quite sensitive to supercell size and k-point density. An uncertainty of $\pm 0.55k_B$ can be estimated for $S^a_{\rm el}$ at T_m, according to the difference with the $N=16$ result. The values of $S^m_{\rm el}$ and $S^f_{\rm el}$, when calculated using the Kohn-Sham eigenstates obtained from the ground-state calculation — instead of the finite-temperature LDA eigenstates — are almost the same (within approximately $0.02k_B$), provided that the Fermi level is calculated again at each temperature, and not taken equal to the ground-state value. This approximation turns out to be also excellent for the calculation of $\Delta H^f_{\rm el}$ and $\Delta H^m_{\rm el}$, with an accuracy better than 0.01 eV.

TABLE II. Calculated formation Ω^f and migration Ω^m volumes at zero temperature and zero pressure, expressed in units of atomic volume Ω_0.

N	n_k	Ω^f	Ω^m
16	20	0.62	
27	8	0.64	
54	4	0.62	0.05

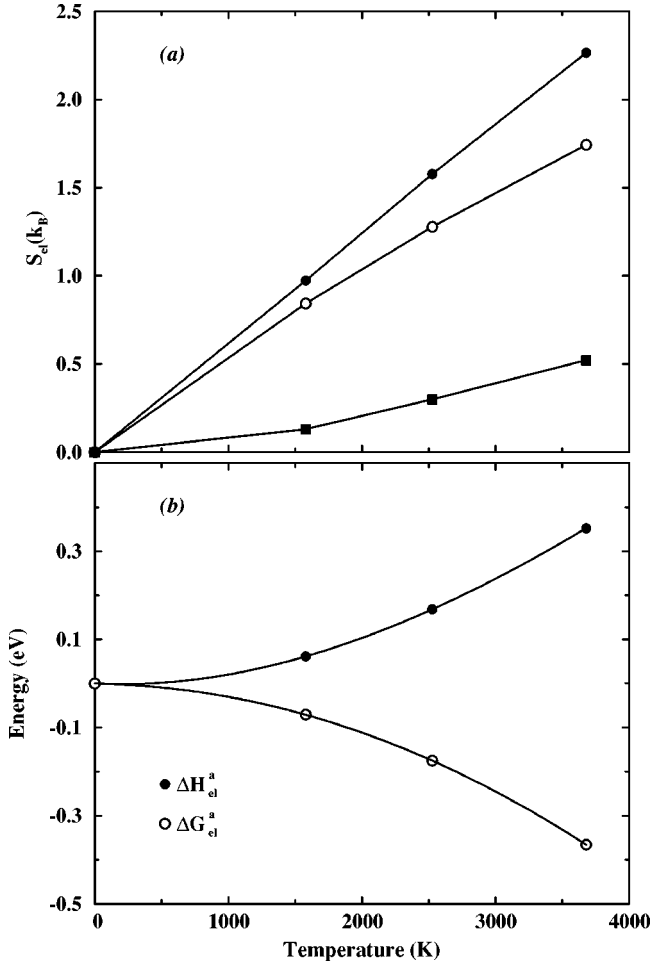

FIG. 2. Effect of electronic excitations on the temperature dependence of vacancy parameters. (a) $S^m_{\rm el}$ (filled squares), $S^f_{\rm el}$ (open circles), and $S^a_{\rm el}$ (filled circles). (b) $\Delta H^a_{\rm el}$ (filled circles) and $\Delta G^a_{\rm el}$ (open circles). Results are presented for calculations with $N=27$ and $n_k=14$ performed using finite electron-temperature LDA on fully relaxed configurations. Lines between symbols are a guide for the eye.

The temperature dependence of $S^f_{\rm el}$, which is positive and almost linear leads to a quadratic and positive (respectively, negative) temperature dependence of $\Delta H^f_{\rm el}$ (respectively, $\Delta G^f_{\rm el}$). The situation is the same for the migration and therefore for the activation functions, as illustrated in Fig. 2(b).

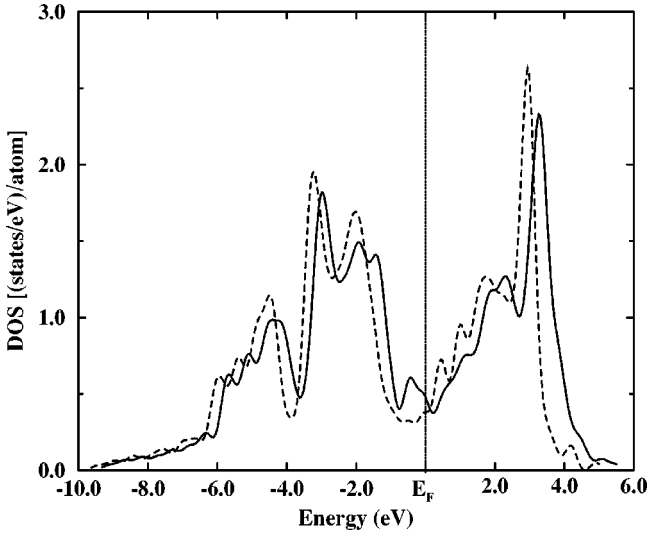

FIG. 3. Density of states for the $N=27$ supercell with (solid line) and without (dotted line) vacancy. A Hermite-Gaussian broadening with a smearing width of $\sigma=20$ mRy was applied to the ground-state eigenvalues of the $n_k=14$ calculation for the plots.

The difference between the values at melting temperature and at zero temperature of the activation enthalpy, 0.36 eV, is not negligible compared to the typical accuracy which is expected for diffusion parameters, and compared to the temperature dependence which is discussed from experiments (see Sec. IV D).

C. Origin of large electronic entropy differences

The large value of $S^f_{\rm el}$, found in the present calculation, is related to significant changes in the density of states (DOS) close to the Fermi level E_F around the vacancy, as shown in Fig. 3 where the DOS of the supercell with 26 atoms and one vacancy is compared to the bulk DOS. In addition to the global change in the shape of the DOS, new features are observed: a strong peak appears just below E_F, close to the minimum of the pseudogap. This peak, which corresponds to states which are localized on the sites of the vacancy and of its nearest neighbors, has some strong similarities with peaks in the local density of states of surface atoms for the (100) and (110) surfaces of molybdenum and tungsten, which have been extensively studied both theoretically and experimentally.[49–52] A similar peak has indeed been obtained for these surfaces by tight-binding and *ab initio* electronic structure calculations:[51,52] it is also located just below E_F and has a particularly large intensity in the case of the (100) surface. The picture of resonance states, associated with atomic virtual bound *d* levels,[50] was proposed to explain the origin of the strong central peak observed in these surfaces. By analogy, the peak presently observed, can be associated to such a resonancelike state. Moreover, the environment of an atom nearest neighbor to the vacancy — denoted NNV atom hereafter — can be compared to that of surface atoms. In terms of coordination Z, i.e., number of nearest neighbors, an NNV atom ($Z=7$) is intermediate between a bulk atom ($Z=8$) and a (110) surface atom ($Z=6$), whereas a (100) surface has a significantly lower coordination ($Z=4$). A particularity of the bcc structure, as compared to the fcc structure, is that an NNV atom has no nearest neighbor within the other NNV atoms. Therefore NNV atoms weakly interact among each other. Within the picture of virtual bound levels, this implies weak interference effects, exactly like in the (100) surface where a surface atom has no nearest neighbors within the surface plane, whereas a (110) surface atom has four nearest neighbors within the surface plane.[50] Besides the central peak in the pseudogap, another peak located 1.35 eV below the E_F is also characteristic of the vacancy. These two peaks are also observed in tight-binding *d*-band calculations.[24] The result for $S^m_{\rm el}$ can also be explained from similar further changes, when the migrating atom is placed at the saddle-point configuration, breaking additional symmetries in the system. This large effect of the electronic entropy contribution to S^f and S^m in tungsten was recently predicted from simple *d*-band tight-binding calculations,[23] where this effect is shown to be large and positive in bcc-transition metals only for elements having their Fermi level close to the minimum of the characteristic pseudogap of the density of states, i.e., group-VI elements: Cr, Mo, and W. The sign and amplitude of the present effect can therefore not be generalized to all bcc elements, but only to those of group VI.

D. Comparison with experiments and discussion

Among the bcc metals, tungsten is the element for which the most detailed and most accurate quenching results are provided, leading to reasonable information on vacancy parameters, even if discussions concerning their analysis remain open, as critically shown in Ref. 4. In particular the resistivity-temperature scale represents a problem which has led to different analyses of the same data.[30] Calculated and experimental defect parameters are compared in Table III and discussed below in particular in view of their temperature dependence.

Formation enthalpy. The values of the vacancy formation enthalpy, deduced from quenched-in resistivity measurements, are, respectively, 3.6 ± 0.2 eV (Refs. 28, 29) and 3.5 ± 0.2 eV (Ref. 30), depending whether only one or all the experimental data sets are retained, and provided that the corrected temperature scale is used.[30] They were obtained from high-temperature measurements ($2400\ {\rm K}<T<3400\ {\rm K}$) assuming temperature independence of H^f, and are therefore in fact the finite-temperature averages over this temperature range. We recall that our most reliable result, i.e., for the $N=54$ supercell calculation, is $H^f=3.44$ eV at zero temperature. When performing an average over the temperature range 2400–3400 K of $H(0)+\Delta H^f_{\rm el}(T)$, we find $\langle H^f\rangle_{2400-3400}=3.61$ eV. The agreement with the experiment is excellent and the difference with $H^f(T=0)$ stresses the importance of temperature dependence of H^f.

Formation entropy. An experimental value of $S^f=3.2k_B$ was proposed for the vacancy formation enthalpy in tungtsen.[29] This value was deduced from a combination of field-ion microscopy investigations and quenching resistivity measurements in the temperature range 2350 to 3132 K. Again, this value was obtained assuming temperature independence of the formation parameters, and reflects the average over the temperature range which is considered. By interpolating the present results, a value of $S^f_{\rm el}$ averaged over the same temperature range gives $\langle S^f_{\rm el}\rangle_{2350-3132}=1.37k_B$.

TABLE III. Comparison between experimental and calculated defect parameters. The calculated enthalpies at zero temperature are reported for the $N=54$ calculations. Their variations with temperature, including only ΔH_{el}, as well as the entropies are obtained from the $N=27$ calculations, by extrapolating between the zero-temperature calculations and the three finite electron-temperature calculations. Their average is then taken in the temperature interval which is considered. Temperatures are expressed in Kelvins.

		Present work	Experiments
H^f (eV)	$T=0$	3.44	
	$2400 \leqslant T \leqslant 3400$	3.61	3.61 ± 0.2[a]
	$2400 \leqslant T \leqslant 3400$		3.51 ± 0.2[b]
$S^f_{el}(k_B)$	$2350 \leqslant T \leqslant 3132$	1.37	
$S^f(k_B)$	$2350 \leqslant T \leqslant 3132$		3.2[c]
H^m (eV)	$T=900$	1.82	1.70 ± 0.1[d]
	$T=2600$	1.86	2.02[d]
H^a (eV)	$T=0$	5.26	
Q_1 (eV)	$T \to 0$		5.60 ± 0.21[e]
	$T \to 0$		5.39 ± 0.34[e]
	$T \to 0$		5.20 ± 0.2[f]

[a]References 28 and 29.
[b]Reference 30.
[c]Reference 29.
[d]Reference 8.
[e]Low-temperature activation energy deduced from measurements from 1700 to 3400 K of Ref. 27 analyzed in Ref. 31.
[f]Low-temperature activation energy deduced from measurements from 2042 to 2819 K of Ref. 54 analyzed in Ref. 31.

This suggests that part of the large experimental value of S^f at high temperatures is due to the electronic contribution. Moreover, by combining the experimental result with our calculated value of S^f_{el}, we deduce a value of $S^f_{vib} \approx 1.83 k_B$, the latter being perfectly consistent with typical values. In a recent discussion on the temperature dependence of vacancy formation parameters in metals, and in particular in tungsten, evidences were given for large values of S^f with a linear temperature dependence.[53] We show that the electronic contribution is a good candidate to explain part of such an effect. This contribution is particularly relevant in tungsten, with a positive sign and a large value at high temperatures.

Migration enthalpy. The vacancy migration enthalpy in tungsten was measured by the change-of-slope method at ~ 900 K.[28] The result of $H^m=1.78$ eV must be corrected according to the temperature scale of Mundy,[30] to $H^m=1.70 \pm 0.1$ eV.[8] The $N=54$ supercell result at zero temperature, $H^m=1.82$ eV, is in excellent agreement with this low-temperature experimental result. The behavior at high temperatures was then investigated by quenched-in resistivity measurements from 1550 to 2600 K.[8] The migration enthalpy was shown to be temperature dependent. A fit, performed assuming a *linear* temperature dependence for H^m, gives $H^m=1.68$ eV at 1550 K and $H^m=2.02$ eV at 2600 K.[8] We have reanalyzed these experimental data assuming a *quadratic* dependence of H^m, i.e., a *linear* temperature dependence of S^m. An equally good fit is obtained, leading to almost the same values in the temperature range 1550–2600 K, i.e., from $H^m=1.69$ eV to $H^m=2.03$ eV. When extrapolated to zero temperatures, these two fits lead to very different values: $H^m=1.18$ eV for the linear fit and $H^m=1.50$ eV for the quadratic fit. We note that both the experimental data at 900 K and the calculated data at zero temperature are more consistent with a quadratic temperature dependence of H^m. Part of this quadratic temperature dependence can be associated with the electronic entropy. However, according to the present calculation, S^m_{el} accounts only for approximately one tenth of the experimentally observed temperature dependence of H^m.

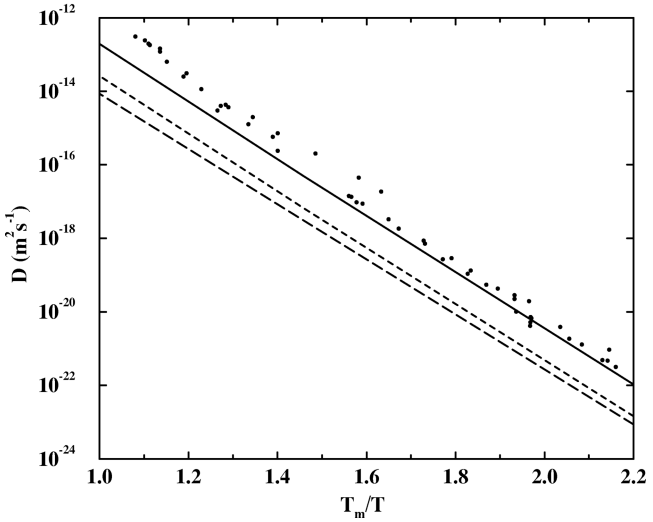

FIG. 4. Tracer self-diffusion coefficient in tungsten: experimental data (filled dots) and theoretical values (solid line) obtained including the calculated value of S^a_{el} and an estimate of S^a_{vib} ($\sim 2k_B$). The theoretical results obtained when only S^a_{el} is considered (dotted line), and when both S^a_{el} and S^a_{vib} are omitted and H^f and H^m are considered temperature independent (dashed line) are shown for comparison. The inverse temperature is normalized to the melting temperature of tungsten, $T_m=3683$ K. All calculated data are taken from the $N=27$ calculations.

Activation energy. The most reliable investigation of self-diffusion coefficient D^* in tungsten was performed by Mundy *et al.*[27] from 1700 to 3400 K. The uncertainties in the experimental measurements were discussed by Neuman *et al.*:[31] they arise mainly from the inaccuracy of the temperature measurement. When a standard fit of $D^*(T)$ as a sum of two exponentials is performed, it was shown[31] that the value of the low-temperature activation energy Q_1 can vary from $Q_1=5.39 \pm 0.34$ eV to $Q_1=5.60 \pm 0.21$ eV depending on which data are decided to be omitted from the fit.[31] The same fit performed on the data of other diffusion coefficient measurements by Arkhipova *et al.* between 2042 and 2819 K gives $Q_1=5.20 \pm 0.46$ eV.[54,31] The significant scatter in the above-mentioned values of Q_1, together with the fact that all measurements were performed at temperatures above 1700 K, make it difficult to extract an accurate asymptotic value of the self-diffusion activation energy at very low temperatures. The self-diffusion activation enthalpy at zero temperature deduced from the present calculations, $H^a=5.26$ eV, is very close to the above experimental values of Q_1, and strongly support the monovacancy mechanism. The absolute values of the self-diffusion coefficient are compared in Sec. IV E.

Formation and migration volumes. No experimental values are available of the formation and migration volumes in tungsten. The present result, $\Omega^f = 0.62\Omega_0$ is slightly larger than the values found in Li and Na from first principles calculations, i.e., $\Omega^f = 0.49\,\Omega_0$ and $0.5\Omega_0$.[12,55] The low value found for the migration volume, i.e., $\Omega^m = 0.05\Omega_0$, is consistent with first principles calculations in Li and Na where they are even found to be negative at zero pressure ($\Omega^m = -0.2\Omega_0$ and $-0.01\Omega_0$, respectively).[55]

E. Self-diffusion coefficient

In this section the tracer self-diffusion coefficient for the monovacancy mechanism $D^*(T)$ is calculated according to Eq. (9) using $\Gamma_0 = \sqrt{\frac{3}{5}}\nu_D$ and $S^m_{\rm vib} = 0$, as explained in Sec. II B. The only unknown quantity is the vibrational contribution to the formation entropy. A typical value for metals is adopted, i.e., $S^f_{\rm vib} = 2k_B$ (Ref. 56). In Eqs. (1) and (7) the finite electron-temperature values of the formation and migration Gibbs energies are used. The results of the present calculation are in excellent agreement with experiments. Figure 4 shows clearly the significant effect of the electronic entropy on the absolute value of the self-diffusion coefficient which is shifted upward almost by one order of magnitude at the melting temperature. Moreover, the temperature dependence of $S^a_{\rm el}$ and therefore of the activation energy induces a small upward curvature. This curvature is not sufficient to account for the whole curvature observed experimentally but has the correct sign and is not negligible. The difference at high temperatures between the experimental data and the calculated curve could be due to a second diffusion mechanism. The possible anharmonic contribution to $S^f_{\rm vib}$ should however also be considered, in particular since they were shown to be important and temperature dependent for the bulk entropy in tungsten.[32]

V. CONCLUSIONS

The vacancy formation and migration energies in tungsten have been calculated using *ab initio* pseudopotential techniques and the LDA formalism at finite electron temperature. The low-temperature values of the formation enthalpy, migration enthalpy, and activation enthalpy, are in excellent agreement with experiments. The electronic contributions to the formation and migration entropies are shown to be important at high temperatures. Moreover their linear temperature dependence is at the origin of a quadratic temperature dependence of the enthalpies and explains part of the experimentally observed temperature dependence of the migration enthalpy and self-diffusion activation energy. A similar effect is expected for other group VI elements (Cr and Mo). The tracer self-diffusion coefficient is calculated within the rate theory: the Arrhenius slope is in excellent agreement with experiments, and so are the absolute values provided that the electronic entropies are taken into account.

[1] J. L. Bocquet, G. Brebec, and Y. Limoge, in *Physical Metallurgy*, edited by R. W. Kahn and P. Haasen (Elsevier, Amsterdam, 1996), p. 536.
[2] J. N. Mundy, Defect Diffus. Forum **83**, 1 (1992).
[3] U. Köhler and C. Herzig, Philos. Mag. A **58**, 769 (1988).
[4] H. Schultz, in *Atomic Defects in Metals*, Landolt Börnstein, New Series, group III, edited by H. Ullmaier (Springer, Berlin, 1991), Vol. 25, p. 115.
[5] A. Seeger, Defect Diffus. Forum **95-98**, 147 (1993).
[6] W. Petry, A. Heiming, J. Trampenau, and G. Vogl, Defect Diffus. Forum **66-69**, 157 (1989).
[7] P. A. Varotsos and K. D. Alexopoulos, *Thermodynamics of Points Defects and their Relation with Bulk Properties* (North-Holland, Amsterdam, 1986).
[8] J. N. Mundy, S. T. Ockers, and L. C. Smedskjaer, Philos. Mag. A **56**, 861 (1987); Mater. Sci. Forum **15-18**, 188 (1987).
[9] A. Da Fano and G. Jacucci, Phys. Rev. Lett. **39**, 950 (1977).
[10] N. V. Doan and Y. Adda, Mater. Sci. Forum **15-18**, 403 (1987); Philos. Mag. A **56**, 269 (1987).
[11] G. Jacucci and R. Taylor, J. Phys. F **9**, 1489 (1979).
[12] W. Frank, U. Breier, C. Elsässer, and M. Fähnle, Phys. Rev. B **48**, 7676 (1993).
[13] U. Breier, W. Frank, C. Elsässer, M. Fähnle, and A. Seeger, Phys. Rev. B **50**, 5928 (1994).
[14] G. H. Vineyard, J. Phys. Chem. Solids **3**, 121 (1957).
[15] C. P. Flynn, in *Point Defects and Diffusion* (Clarendon, Oxford, 1972); Phys. Rev. **171**, 682 (1968).
[16] W. Frank, U. Breier, C. Elsässer, and M. Fähnle, Phys. Rev. Lett. **77**, 518 (1996).
[17] S. M. Foiles, M. I. Baskes, and M. S. Daw, Phys. Rev. B **33**, 7983 (1986).
[18] J. M. Harder and D. J. Bacon, Philos. Mag. A **54**, 651 (1986).
[19] V. Rosato, M. Guillopé, and B. Legrand, Philos. Mag. A **59**, 321 (1989).
[20] F. Willaime and C. Massobrio, in *Defects in Materials*, edited by P. D. Bristowe *et al.*, MRS Symposia Proceedings No. 209 (Materials Research Society, Pittsburgh, 1991), p. 293.
[21] F. Cleri and V. Rosato, Phys. Rev. B **48**, 22 (1993).
[22] Y. Ohta, M. W. Finnis, D. F. Pettifor, and A. P. Sutton, J. Phys. F **17**, L273 (1987).
[23] M. Nastar, Ph.D. thesis, Paris VI University (CEA Report No. R-5685, 1995).
[24] F. Willaime (unpublished).
[25] P. H. Dederichs, T. Hoshino, B. Drittler, K. Abraham, and R. Zeller, Physica B **172**, 203 (1991).
[26] T. Korhonen, M. J. Puska, and R. M. Nieminen, Phys. Rev. B **51**, 9526 (1995).
[27] J. N. Mundy, S. J. Rothman, N. Q. Lam, H. A. Hoff, and L. J. Nowicki, Phys. Rev. B **18**, 6566 (1978).
[28] K. D. Rasch, R. W. Siegel, and H. Schultz, Philos. Mag. A **1**, 91 (1980).
[29] J. Y. Park, H. C. W. Huang, R. W. Siegel, and R. W. Balluffi, Philos. Mag. A **48**, 397 (1983).
[30] J. N. Mundy, Philos. Mag. A **46**, 345 (1982).
[31] G. Neuman and V. Tölle, Philos. Mag. A **61**, 563 (1990).
[32] O. Eriksson, J. M. Wills, and D. Wallace, Phys. Rev. B **46**, 5221 (1992).

[33] R. D. Hatcher, R. Zeller, and P. H. Dederichs, Phys. Rev. B **19**, 5083 (1979).
[34] D. R. Hamann, M. Schlüter, and C. Chiang, Phys. Rev. Lett. **43**, 1494 (1979).
[35] G. B. Bachelet, D. R. Hamann, and M. Schlüter, Phys. Rev. B **26**, 4199 (1982).
[36] C. Bungaro, S. de Gironcoli, and S. Baroni, Phys. Rev. Lett. **77**, 2491 (1996).
[37] D. J. Chadi and M. L. Cohen, Phys. Rev. B **8**, 5747 (1973); H. J. Monkhorst and J. D. Pack, *ibid.* **13**, 5188 (1976).
[38] N. D. Mermin, Phys. Rev. **A137**, 1441 (1965).
[39] J. Callaway and N. H. March, Solid State Phys.: *Advances in Research and Applications*, edited by H. Ehrenreich, D. Turnbull, and F. Seitz (Academic, New York, 1984), Vol. 38, p. 136.
[40] M. J. Gillan, J. Phys.: Condens. Matter **1**, 689 (1989).
[41] F. Perrot and M. W. C. Dharma-Wardana, Phys. Rev. A **30**, 2619 (1984).
[42] R. E. Watson and M. Weinert, Phys. Rev. B **30**, 1641 (1984).
[43] E. G. Moroni, G. Grimvall, and T. Jarlborg, Phys. Rev. Lett. **76**, 2758 (1996).
[44] M. Methfessel and A. T. Paxton, Phys. Rev. B **40**, 3616 (1989).
[45] S. de Gironcoli, Phys. Rev. B **51**, 6773 (1995).
[46] A. De Vita and M. J. Gillan, J. Phys.: Condens. Matter **3**, 6225 (1991).
[47] M. Methfessel, C. O. Rodriguez, and O. K. Andersen, Phys. Rev. B **40**, 2009 (1989).
[48] C. C. Matthai and D. J. Bacon, Philos. Mag. A **52**, 1 (1985).
[49] S.-L. Weng, E. W. Plummer, and T. Gustafsson, Phys. Rev. B **18**, 1718 (1978).
[50] J. Friedel, J. Phys. (Paris) **37**, 883 (1976).
[51] M. C. Desjonquères and F. Cyrot-Lackmann, J. Phys. F **6**, 567 (1976).
[52] M. Posternak, H. Krakauer, A. J. Freeman, and D. D. Koelling, Phys. Rev. B **21**, 5601 (1980).
[53] Y. Kraftmakher, Philos. Mag. A **74**, 811 (1996).
[54] N. K. Arkhipova, S. M. Klotsman, S. M. Rabovskiy, A. Ya, and A. N. Timofeyev, Fiz. Met. Metalloved. **43**, 779 (1977).
[55] U. Breier, V. Schott, and M. Fähnle, Phys. Rev. B **55**, 5772 (1997).
[56] G. Grimvall, *Thermodynamical Properties of Materials* (North-Holland, Amsterdam, 1986).